

New Implementation of Mm-Wave Heterodyne Receiver Based on Six-Port Technology: Circuit Characterization and High Data-Rate Demodulation Results

Djilali Hammou^{1, *}, Mourad Nedil¹, and Serioja O. Tatu²

Abstract—This paper presents a new implementation of a millimeter wave heterodyne receiver based on six-port technology. The six-port circuit is designed using three hybrid couplers H-90° and a new ring power divider. For the characterization of the circuit, several six-port two-port measurement configurations were designed and fabricated on the same wafer along with calibration standards. The new six-port architecture evaluation based on q_i points location demonstrates wideband performances and high coupled-port phase and amplitude balance in the 57–65 GHz frequency band. The six-port model based on S -parameter measurements is then implemented in ADS software, for realistic advanced simulation systems of a short-range 60 GHz wireless link. The millimeter wave frequency conversion is performed using a six-port down-converter. The second frequency conversion uses conventional means due to the low IF frequency value. The demodulation results of a V-band QPSK signal for high data rate from 100 to 1000 Mbits/s are presented and discussed. The results of the Bit Error Rate (BER) analysis demonstrate that the proposed architecture can be successfully used for high speed wireless link transmission at 60 GHz.

1. INTRODUCTION

The millimeter wave spectrum is nowadays an unavoidable candidate to ensure multi-gigabit/s data links [1–4]. In this area, the use of millimeter wave frequencies enables the design of compact and low-cost wireless millimeter wave communication front-ends, which can offer convenient terminal mobility and high capacity channels.

The six-port technology, widely recognized in microwave low-cost circuit characterizations [5–9] has been used as an unconventional technique to perform frequency down-conversion [10–17]. The millimeter wave frequency conversion is performed using a passive circuit, multiport, and related power detectors, avoiding the conventional millimeter-wave active costly mixers.

The Monolithic Microwave Integrated Circuit technology is used in large scale production, and the Miniaturized Hybrid Microwave Integrated Circuit is appropriate for prototyping and small to medium scale production. Initial design and circuit characterization results of several new passive circuits for advanced millimeter wave systems have been recently reported [18–20].

In this contribution, a millimeter wave heterodyne receiver based on new six-port implementation is proposed for high-speed wireless communication systems. A broadband six-port circuit that can support data-rates up to quasi-optical speeds is then needed. In this work we propose a six-port architecture constructed with a new ring power divider and three rounded hybrid couplers H-90°. The new power divider design reduces the inherent undesirable mutual coupling between the transformer

Received 28 January 2016, Accepted 13 May 2016, Scheduled 3 July 2016

* Corresponding author: Djilali Hammou (djilali.hammou@uqat.ca).

¹ Engineering School, LRTCS, University of Quebec in Abitibi-Temiscamingue (UQAT), Canada. ² Institut National de la Recherche Scientifique, INRS-EMT, 800, de la Gauchetière Ouest, R 6900, Montréal, QC., H5A 1K6, Canada.

arms of the conventional power divider at millimeter wave frequencies and then, improve the six-port circuit performances over the considered 60 GHz frequency band. The circuit architecture design and characterization and demodulation results are analyzed in Section 3.

2. BASIC MHMIC CIRCUITS CHARACTERIZATION

The integration of the millimeter-wave multi-port front-end on ceramic substrate needs the full characterization of each basic circuit, such as couplers, antennas, power dividers/combiners, and power detectors.

The most robust and popular technique is the thru-reflect-line (TRL) calibration, well suited for on-wafer measurements at millimeter wave frequencies [21, 22]. It is based on transmission-line calibration standards which include non-zero length thru, reflect (open or short), and delay line standards. In order to ensure calibration and subsequent measurement accuracy, the TRL (Through Reflect Line) calibration standards are designed and fabricated on the same alumina substrate as the devices under test (DUT). The TRL calibration kit is presented in Fig. 1(a). The length difference between the through and the line standards, Δl , is calculated to cover the frequency band of interest, without phase ambiguity. On the other hand, to provide connection with GSG 150 μm probes, CPWG to microstrip transitions have been designed and included. Fig. 1(b) exhibits the circuit under measurement using 150 GSG coplanar probes, connected through WR-12 waveguides at millimeter wave modules.

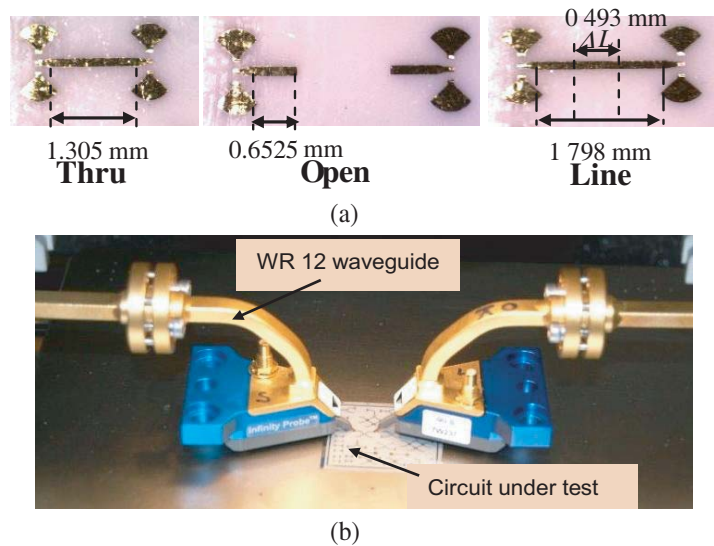


Figure 1. (a) Micro-photograph of the on-wafer TRL calibration standards designed for 150 μm coplanar pico-probes. (b) MHMIC circuit characterization using 150 GSG coplanar probes connected through WR-12 waveguides.

3. MILLIMETER WAVE SIX-PORT CIRCUIT

3.1. Circuit Design and Characterization

The six-port circuit was first developed by Cohn and Weinhouse [5] to evaluate the phase of a microwave signal. It was extended in the 1970's by Engen and Hoer [6–9] for accurate automated measurements of the complex reflection coefficient in microwave network analysis.

Since 1993, the six-port techniques have been further expanded and developed for direct modulation and demodulation of microwave signals [10–17].

Basically, the six-port circuit is a passive circuit, composed of several couplers, interconnected by transmission lines and phase shifters. It has two inputs and four outputs and acts as an interferometer;

its output signals are linear combinations of phase shifted reference and input unknown signals. By using power detectors connected to output ports followed by analog or digital signal processing of the output baseband signals, this circuit provides high precision of relative phase and amplitude measurements.

Various six-port architectures exist in literature. The most known is composed of a 3 dB Wilkinson power divider and three 90° hybrid couplers. However, at high frequencies, the two branches of the conventional Wilkinson power divider must be placed very close to each other to be connected to the $100\ \Omega$ resistor [24, 25] couplers and a power divider. This leads to a strong undesirable mutual coupling between the output lines [24–26].

The proposed approach is to design broadband six-port circuits that could support data-rates up to quasi-optical speeds and avoid calibration procedures. In order to improve the six-port circuit performances over an ultra-wide band of several GHz, the ring power divider designed in [26] is used instead of the Wilkinson power divider. As illustrated in Fig. 2, this design enhances the traditional Wilkinson design by adding two half-wave transmission lines to connect the integrated resistor. These additional lines of $\lambda_g/2$ electric lengths create an ideal framework for the isolation resistor, overcoming undesirable mutual coupling between the transformer arms.

According to the performance results of the hybrid coupler H- 90° [20, 21], the ring power divider [26] and the recent progress in circuit design and characterization [27], a new six-port implementation is designed and fabricated.

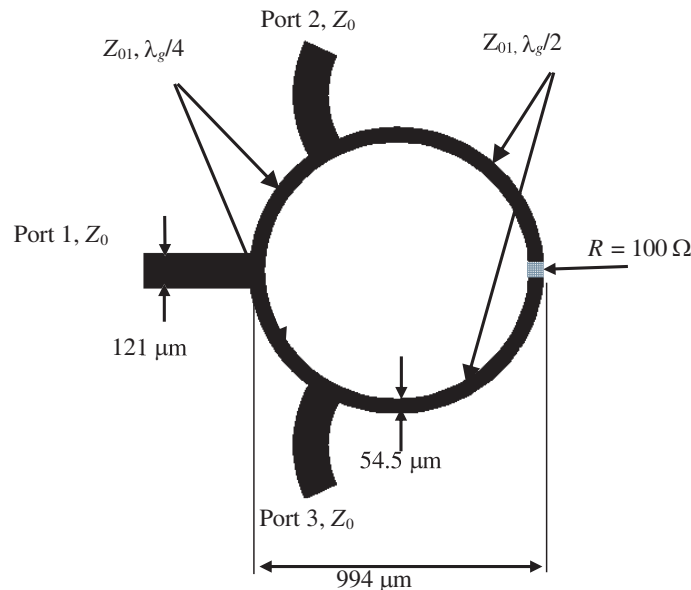


Figure 2. Layout of new ring power divider/combiner.

As depicted in Fig. 3, several two-port configuration measurements of this circuit are designed and fabricated along with the TRL calibration kit to perform on-wafer millimeter wave characterization. We use a customized probe station and VNA. The millimeter wave VNA includes the E 8362 PNA Network Analyzer and the N 5260A Millimeter Wave Head Controller from Agilent Technologies. Two millimeter wave extenders, from OML Inc., optimized for Agilent N 5260A, are used for WR 12 waveguide operation (60–90 GHz). Taking into account huge attenuation on millimeter wave cables, this ensures very high dynamic range measurements. The S -parameter measurements are performed starting from 60 GHz. This is inherent to the measurement setup capabilities as described below. However, it is possible to extrapolate these results below this frequency, to cover the frequency bandwidth for 60 GHz communication applications, from 57 to 65 GHz.

The design criterion of a six-port consists of achieving a specific distribution of the q_i points [5–7]. In fact, a high performance interferometry is achieved when q_i points are equidistant from the origin of the complex coordinate system and angularly spaced by 360° divided by their number ($i = 4$ in this case). When the RF and LO ports are isolated, the q_i points of the six-port are expressed in terms of

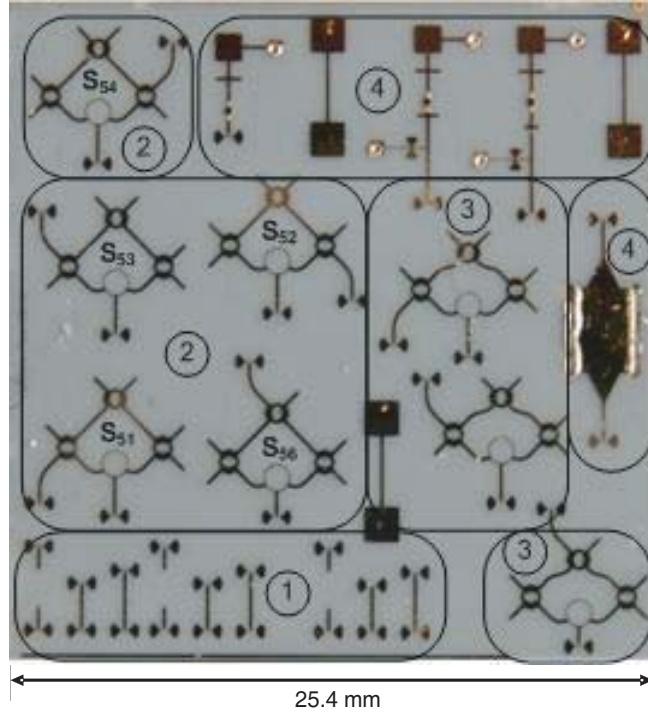


Figure 3. Micro-photograph of the fabricated ceramic wafer for six-port circuit characterization: (1) TRL calibration kits; (2) Six-port circuit in S_{51} , S_{52} , S_{53} , S_{54} and S_{26} measurement configurations; (3) Rounded arms six-port's measurement configurations; (4) Other circuits with $50\ \Omega$ test circuit.

S -parameters as follows:

$$q_i = \frac{S_{i5}}{S_{i6}} \quad i = 1, 2, 3, 4 \quad (1)$$

The q_i point's distribution in the complex coordinate plane of an ideal six-port is as follows: $\frac{1}{\sqrt{2}}(1 - j)$; $\frac{1}{\sqrt{2}}(1 + j)$; $\frac{1}{\sqrt{2}}(-1 - j)$ and $\frac{1}{\sqrt{2}}(-1 + j)$.

The calculated frequency dependent q_i points based on S -parameter measurements and simulations along with ideal distribution marked as (x) are plotted in Fig. 4.

Good agreement between measurements and simulations is obtained, as shown in the dashed-line highlighted point location. These results demonstrate high q_i points' location accuracy over the whole considered frequency band (60 to 65 GHz). Indeed, the magnitudes of the q_i points are equal and close to 1, while the argument difference is close to 90° between two corresponding q_i points. As a result, the proposed six-port architecture presents high factor amplitude and phase balance over an ultra-wideband, while maintaining a high isolation and matching RF inputs.

Furthermore, parameters, such as RF input matching, power transmission and phase balance, are also investigated and plotted in the frequency band of interest. These results are illustrated in Fig. 5, where good agreement between measurements and simulations is observed.

As revealed in Fig. 5(a), the RF input port 5 is well matched; the return loss is better than -15 dB in the whole frequency band.

The transmission coefficient measurements S_{5i} where $i = 1$ to 4 is close to the expected -6 dB. Indeed, less than 0.5 dB of additional loss is obtained. Due to perfect symmetry from port 5, and not overcrowding the plots, we have represented here only S_{52} . The phase performance $Phase_{5i}$, represented in Fig. 5(b), shows two quasi-parallel characteristics. The phase difference between two adjacent ports is close to the expected quadrature reference of 90° . Indeed, the phase imbalance $\Delta phase_{S_{5i},j}$ does not exceed 6° , over the considered frequency band.

Moreover, the performance of the proposed six-port architecture is compared with previous and

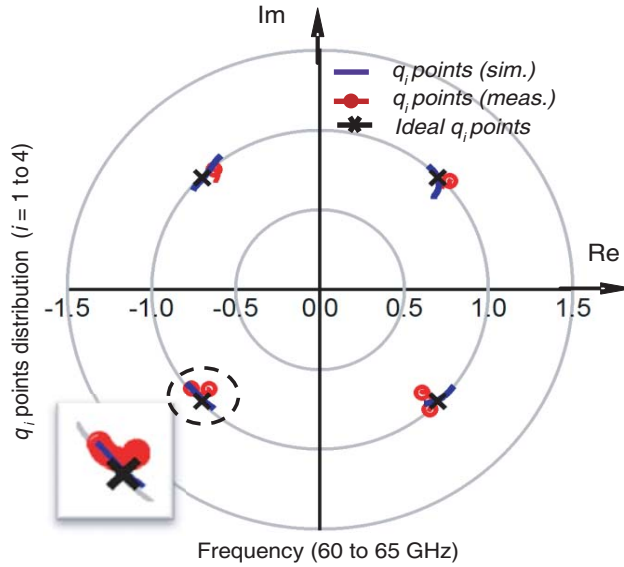


Figure 4. Polar plot of the measured, simulated and ideal q_i points distributions of the proposed six-port circuit.

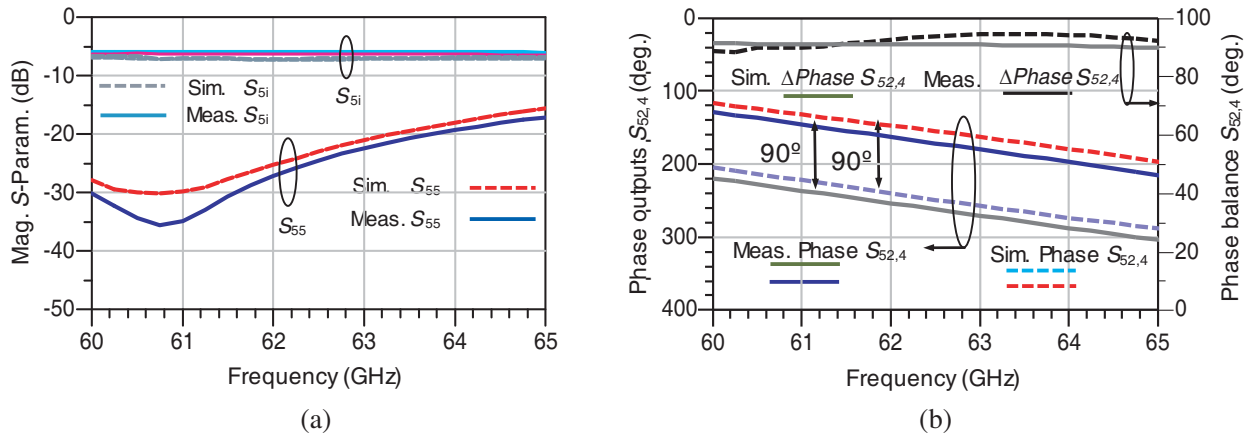


Figure 5. S -parameter measurements and simulations of the proposed six-port circuit; (a) RF input matching and transmission; (b) Output phase, $S_{5,2,4}$ between adjacent ports 2 and 4 and phase balance, Phase $S_{5,2,4}$.

related works in the 60 GHz frequency band. These results are shown in Table 1.

The six-port architecture in [28] uses one power divider and three planar Goubau line (PGL) couplers. The simulation results of this circuit is shown in Table 1. As seen, The RF matching is better than 15 dB. However, the amplitude imbalance is near 2 dB while the phase imbalance reaches 10° compared to the expected quadrature reference of 90° .

In [29], the author proposes a miniaturized six-port circuit designed using three compact 3 dB branch-line couplers (BLC) and one compact Wilkinson power divider. The performances of the six-port circuit based on S -parameter simulation results show that the RF matching is better than 15 dB in the whole frequency band. However, the transmission loss is around 8.7 dB from RF port to the output ports.

The six-port circuit proposed in [30] is composed of a Wilkinson power divider and three 90° hybrid couplers. The measured insertion losses of the circuit are 7–8 dB and 8–9 dB for LO and RF excitations, respectively. The amplitude imbalance is around 1 dB at 60 GHz and greater than 1.5 dB over the whole

considered frequency band. The measured phase differences between adjacent output ports are less than 5° at 60 GHz.

The six-port architecture reported in [21] is built with four 90° hybrid couplers. The power divider is realized by one of the 90° hybrid couplers along with a transmission line of 90° . This deteriorates the desired amplitude and phase split ratio over a wide band, raising phase and amplitude imbalance. Indeed, the S -parameter measurements of this architecture show, for the considered coupled ports, a phase imbalance less than 10% over the entire bandwidth. However, the amplitude imbalance reaches 1.5 dB at higher frequencies.

Table 1. Performance comparison of proposed six-port circuit with other related works at 60 GHz.

	Ref. [28]	Ref. [29]	Ref. [30]	Ref. [21]	Proposed Circuit
Return loss (dB)	-20	-15	-15	-20	-20
Transmission loss (dB)	-8	-8.7	-7.5 to -9.5	-7.5	-6.5
Amplitude Imbalance (dB)	≤ 2	1	-20	1.5	0.5
Phase Imbalance (deg.)	≤ 10	Not mention	1.5	≤ 9	≤ 5

High performance results of the proposed six-port are obtained as revealed by Table 1. The measurement results demonstrate that the proposed circuit is suitable for V-band high order data-rate wireless communications systems, using MPSK or MQAM modulations.

3.2. Six-Port Receiver Architecture and Operating Principle

The heterodyne architecture is widely used in wireless communications due to its well-known advantages [31, 32]. However, the main challenge in the millimeter wave domain is the design of a high-quality and low-cost mixer [32]. As illustrated in Fig. 6 and in order to overcome this problem, the receiver uses a six-port millimeter-wave mixer (SPMM) topology, as demonstrated in [33] to perform millimeter-wave down-conversion. The SPMM uses Schottky diodes that act as detectors. This architecture requires reduced LO power, as low as -20 dBm, to perform an efficient frequency conversion in comparison with the quasi-conventional architecture [33].

As shown in Fig. 6, the SPMM inputs are connected to a low-noise amplifier (LNA) and to the first millimeter wave local oscillator (L_{O1}), respectively. The intermediary frequency module (IFM) allows quadrature IF signals to be directly obtained using detected output six-port signals and differential amplifiers. The intermediary frequency module (IFM) allows quadrature IF signals to be directly obtained using detected output six-port signals and differential amplifiers such as the THS4304. It is a wideband, voltage-feedback amplifier designed for the use in high-speed analog signal-processing chains with wideband performance up to 3 GHz at unity gain [34].

Finally, baseband module (BBM) amplifies these signals and sample and hold circuits (SHC) operating at the bit-rate frequency generate improved output demodulated signals.

Mostly, for a multi-port system, the output signals, b_i , can be expressed with the dispersion parameters S_{ij} as follows:

$$b_i = \sum_{j=1}^6 S_{ij} a_j, \quad i = 1 \text{ to } 6 \quad (2)$$

The scattering matrix of the proposed six-port circuit, where the schematic is illustrated in Fig. 7, is obtained using the scattering matrix of a 90° hybrid coupler and of the power divider.

$$[S] = \frac{1}{2} \begin{bmatrix} 0 & 0 & 0 & 0 & -j & j \\ 0 & 0 & 0 & 0 & 1 & j \\ 0 & 0 & 0 & 0 & 1 & 1 \\ 0 & 0 & 0 & 0 & -j & -1 \\ -j & 1 & 1 & -j & 0 & 0 \\ j & j & 1 & -1 & 0 & 0 \end{bmatrix} \quad (3)$$

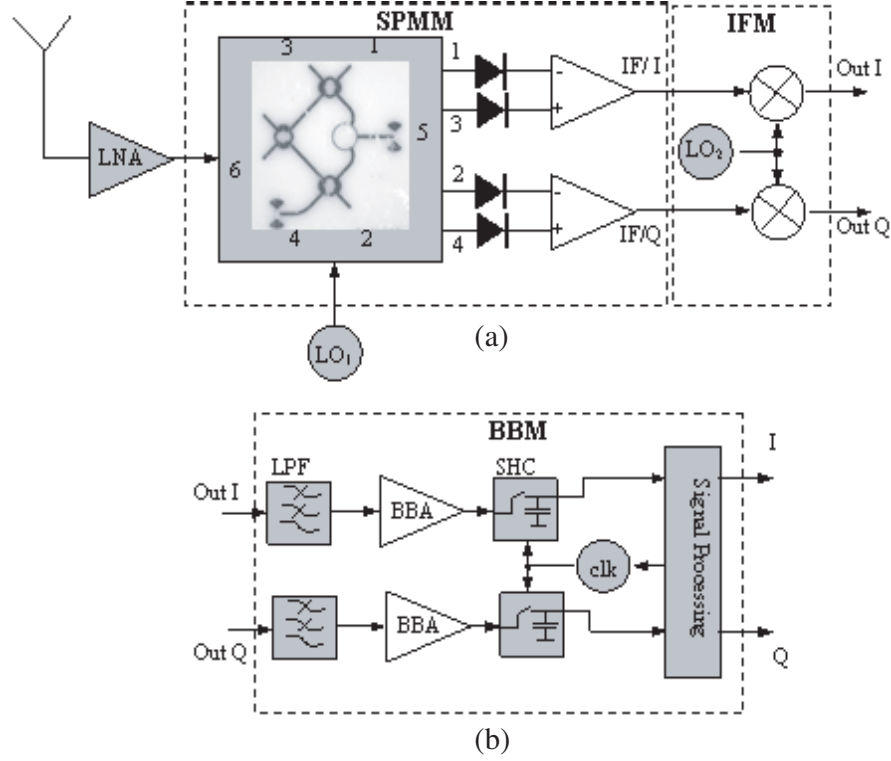


Figure 6. Block diagram of the heterodyne six-port receiver: (a) SPMM and IFM modules; (b) BBM module.

Let's assume that there are two normalized wave inputs, a_5 from the LO and a_6 from the RF input. These two normalized input waves have an α amplitude ratio, a $\Delta\varphi(t) = \varphi_6(t) - \varphi_5$ phase difference, and a $\Delta\omega = \omega - \omega_0$ frequency shift. They are expressed as follows:

$$a_5 = a \cdot e^{j(\omega_0 \cdot t + \phi_5)} \quad (4)$$

$$a_6 = \alpha \cdot a \cdot e^{j(\omega \cdot t + \phi_6(t))} = \alpha \cdot a_5 \cdot e^{j(\Delta\omega \cdot t + \Delta\phi(t))} \quad (5)$$

We assume a perfect match ($a_1 = a_2 = a_3 = a_4 = 0$); the four normalized output waves can be calculated using Equation (2) and the six-port scattering matrix (3).

$$b_i = a_5 \cdot S_{5i} + a_6 \cdot S_{6i}, \quad i = 1 \text{ to } 4 \quad (6)$$

$$|b_i| = \frac{a}{2} \cdot \left| 1 + \alpha \cdot e^{j[\Delta\omega t + \Delta\phi(t) + (3-i)\frac{\pi}{2}]} \right|, \quad i = 1 \text{ to } 4 \quad (7)$$

In order to obtain the IF output signals, four power detectors are connected to the multi-port outputs. As known, the output voltage of an ideal power detector is proportional to the square magnitude of the RF input signal:

$$v_i = K_i \cdot |b_i|^2 = K_i \cdot b_i \cdot b_i^*, \quad i = 1 \text{ to } 4 \quad (8)$$

Supposing that identical power detectors are used, ($K_i = K$, for $i = 1$ to 4), the output voltages become:

$$v_{1,3}(t) = K \frac{a^2}{4} \cdot \{1 + \alpha^2 \mp 2 \cdot \alpha \cdot \cos[\Delta\omega \cdot t + \Delta\phi(t)]\} \quad (9)$$

$$v_{2,4}(t) = K \frac{a^2}{4} \cdot \{1 + \alpha^2 \mp 2 \cdot \alpha \cdot \sin[\Delta\omega \cdot t + \Delta\phi(t)]\} \quad (10)$$

As seen, the output voltages at the pair of ports 1 and 3, and 2 and 4, respectively, are phase opposites. Therefore, the quadrature output signals can be obtained using two differential amplifiers at the outputs

of the SPMM stage

$$v_{IF}^I(t) = A_{IF} \cdot [v_3(t) - v_1(t)] = \alpha \cdot K \cdot a^2 \cdot A_{IF} \cdot \cos[\Delta\omega \cdot t + \Delta\phi(t)] \quad (11)$$

$$v_{IF}^Q(t) = A_{IF} \cdot [v_4(t) - v_2(t)] = \alpha \cdot K \cdot a^2 \cdot A_{IF} \cdot \sin[\Delta\omega \cdot t + \Delta\phi(t)] \quad (12)$$

Finally, after the second frequency conversion and low pass filtering, the obtained output I/Q signals are expressed as:

$$I(t) = \frac{1}{2} \cdot \alpha \cdot a^2 \cdot K \cdot A_{IF} \cdot A_{BB} \cdot \cos(\Delta\phi(t)) \quad (13)$$

$$Q(t) = \frac{1}{2} \cdot \alpha \cdot a^2 \cdot K \cdot A_{IF} \cdot A_{BB} \cdot \sin(\Delta\phi(t)) \quad (14)$$

These pairs of equations depend on the information related to amplitude ratio (α), phase difference ($\Delta\phi(t)$) and frequency shift. Thus, the proposed heterodyne receiver based on the new six-port architecture can demodulate arbitrary PSK, QPSK, MPSK and MQAM modulation schemes.

4. DEMODULATION RESULTS FOR THE HETERODYNE SIX-PORT RECEIVER

In order to perform realistic simulations in ADS platform and to evaluate demodulation performances, the proposed six-port circuit model of Section 3 is used as illustrated in Fig. 6.

Envelope simulations are performed using pseudo-random QPSK modulated signals. The transmitter uses a vector modulator and two pseudo-random sources (I and Q input signals) having two different voltage levels of ± 1 V. The carrier consists of a 61 GHz V-band signal, and it is modulated in the range between 100 and 1000 Mb/s. The propagation path simulation is performed using the Friis model, and the receiver uses the block diagram of Fig. 6.

According to the well-known Friis equation [35], the free space LOS attenuation is equal to 88 dB for $d = 10$ m range. In this system analysis, the antenna gains are set at 10 dBi. The LNA gain and noise figure (NF) are 21 dB, and 3.8 dB, respectively, a common value for today's 60 GHz integrated

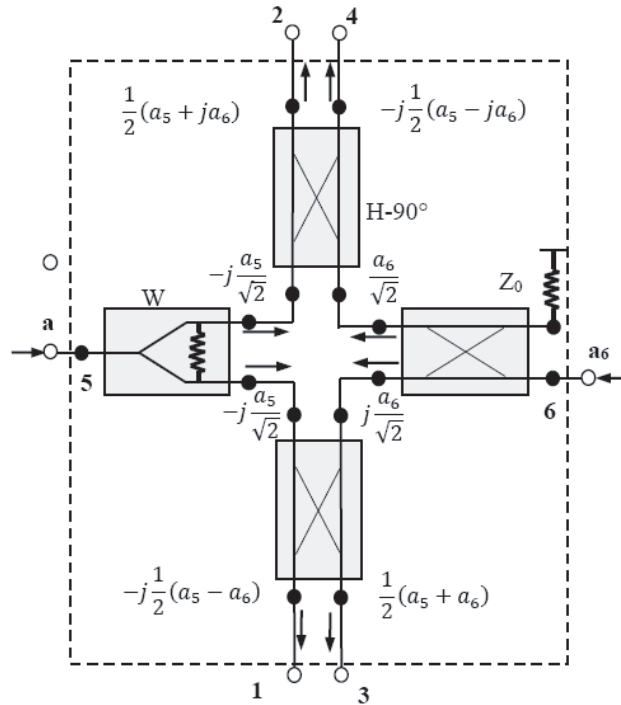


Figure 7. Six-port circuit schematic using 3 hybrid couplers ($H-90^\circ$) and a Wilkinson power divider (W). Input ports: Port 5 (LO) and Port 6 (RF); Output ports: Port 1, Port 2, Port 3 and Port 4.

amplifiers such as HMC-ALH382 from Hittite Microwave Corporation. The millimeter wave power detector models are based on the Spice model of the zero-bias Schottky diode, model HSCH-9161, of Agilent Technologies.

To obtain data output squared waves, and, consequently, perfect demodulated constellations, limiters are used in the baseband (BB) stage of the receiver. According to future high-speed requirements of the wireless standard IEEE 802.15.3.c, the IF was chosen at 2.5 GHz. The LO is supposed perfectly synchronized, an important advantage of this architecture, compared to the direct conversion. This can be obtained by controlling the lower frequency local oscillator from digital processing block to IFM block (LO₂).

Figures 8 and 9 show typical spectrums respectively, of a quadrature IF signal (I or Q) centered at 2.5 GHz and a baseband quadrature signal (I or Q) obtained after the second down-conversion.

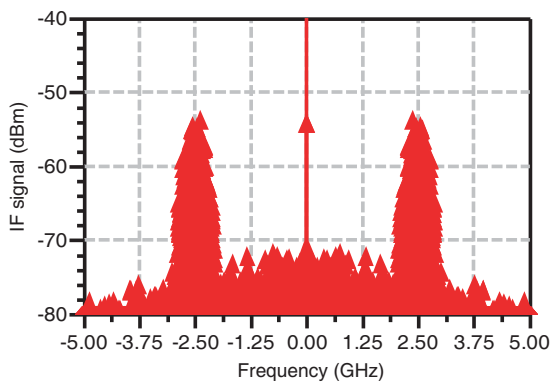


Figure 8. Typical spectrum of a quadrature IF signal (I or Q).

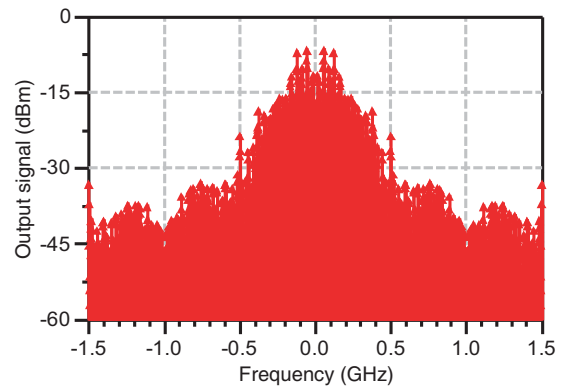


Figure 9. Typical spectrum of a baseband quadrature signal (I or Q).

This result illustrates the six-port performance for a pseudorandom QPSK modulated signals at 1 GB/s to replace a conventional millimeter wave active mixer.

Figure 10 illustrates demodulation results of a pseudo-random QPSK bit sequence of 100 nanoseconds, at 1 Gb/s. As observed, the demodulated signal shapes follow the input quadrature signals generated by the transmitter.

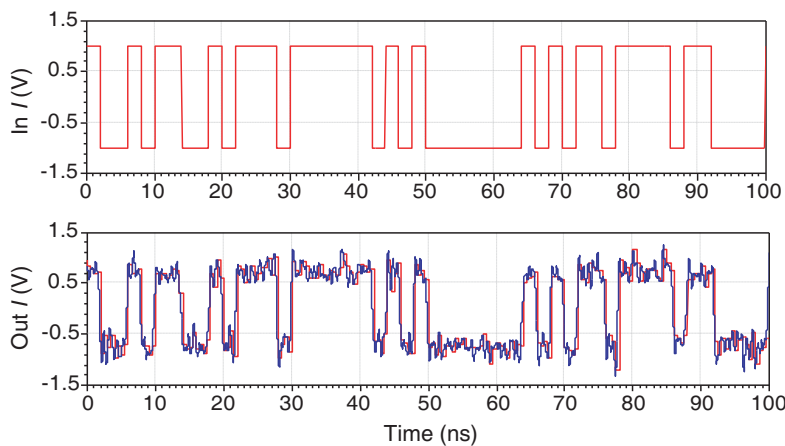


Figure 10. Demodulation results of 1 Gb/s QPSK pseudorandom bit sequence.

To evaluate wireless link quality for a Gb/s pseudo-random QPSK modulated signals, a BER analysis is performed for pseudorandom QPSK modulation data rate between 100 and 1000 Mb/s. Fig. 10 shows the BER results versus the average energy of a modulated bit to the noise power spectral

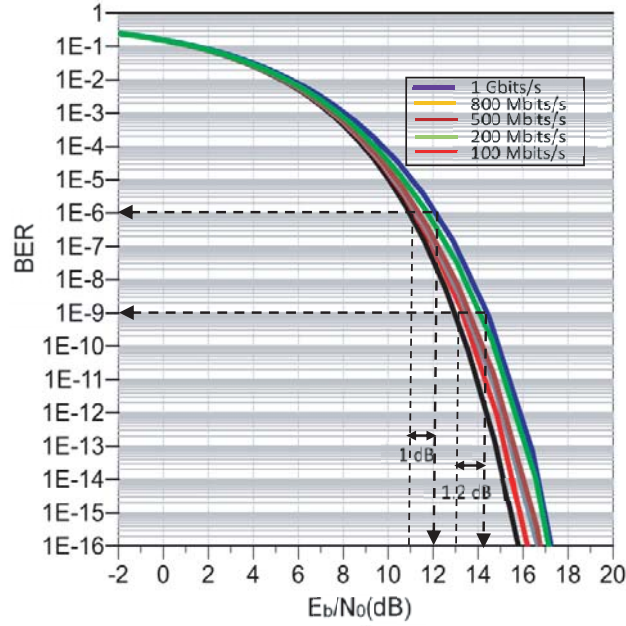


Figure 11. The BER performance for a QPSK modulation data-rate from 100 to 1000 Mb/s.

density (E_b/N_0). As illustrated, simulations show a BER performance better than 10^{-6} for E_b/N_0 ratio around 12 dB in all cases. There is only 1 dB additional shift in E_b/N_0 for 1 Gb/s. This is an excellent result if we consider that it corresponds to the tenfold increase in data rate from 100 Mb/s to 1 Gb/s. To reach a BER of 10^{-9} (required for uncoded HDTV transmission), E_b/N_0 must increase a further 1.2 dB to reach 14.2 dB.

To calculate error vector, we consider the demodulation results of the 1 Gb/s QPSK pseudorandom bit sequence of 100 ns. The baseband signals $\Gamma_{in,n}$ and $\Gamma_{out,n}$ are defined as:

$$\Gamma_{in,n} = I_{in,n} + Q_{in,n} \text{ and } K \cdot \Gamma_{out,n} = K \cdot I_{out,n} + K \cdot Q_{out,n} \quad (15)$$

These vectors represent the transmitted and ideal baseband signals. Constellation normalization is achieved by affecting the output constellation $\Gamma_{out,n}$ with a K coefficient to correlate the symbols in the two constellations [36]. Thus, EVM is defined as the root-mean-square (RMS) value of the difference between simulated symbols and ideal symbols:

$$EVM(\%) = \sqrt{\frac{\frac{1}{N} \sum_{n=1}^N |\Gamma_{in,n} - K \cdot \Gamma_{out,n}|^2}{|\Gamma_{in}|^2}} \cdot 100 \quad (16)$$

where N is the number of symbols.

Figure 12 shows the EVM-per-symbol calculations for a pseudorandom QPSK bit sequence of 100 ns at 1 Gb/s. The effective EVM corresponds to the mean of the EVM-per-symbol with 100 ns bit

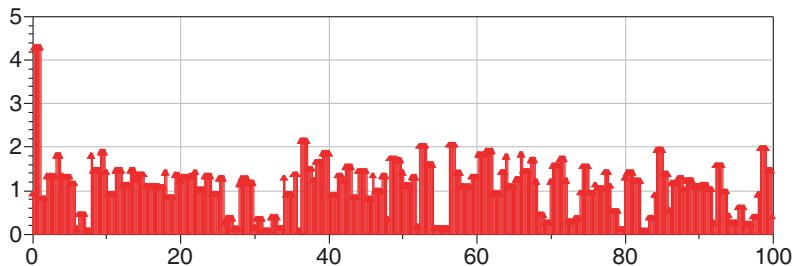


Figure 12. EVM-per-symbol for a 100 ns transmitted bit sequence at 1 Gb/s.

sequence length. As seen, this result is under 2%, which corroborates the BER results in the previous paragraph and settles the capability of the six-port heterodyne receiver for the millimeter-wave wireless high data-rate communications systems.

5. CONCLUSION

A new millimeter wave heterodyne architecture receiver based on six-port technology has been presented in this paper. In order to obtain millimeter-wave frequency conversion, this receiver uses the specific properties of the new the six-port circuit, avoiding the use of a conventional diode based on a costly active mixer.

Realistic simulation systems of a short-range 60 GHz wireless link were performed, using a measurement based on a six-port model and a QPSK modulated signal of 1 Gb/s. These demodulation results are validated by BER calculation.

The proposed six-port heterodyne architecture enables the design of compact and low-cost wireless millimeter-wave communication receivers for future high-speed wireless communication systems.

ACKNOWLEDGMENT

The authors would like to express their gratitude to chief technologist Jules Gauthier (Poly-Grames Research Center, École Polytechnique de Montréal) for his technical assistance.

REFERENCES

1. Federal Communication Commission, Amendment of Parts 2, 15 and 97 of the Commission's Rules to Permit Use of Radio Frequency above 40 GHz for New Radio Applications, FCC 95-499, ET Docket No. 94-124, RM-8308, Dec. 15, 1995.
2. Smulders, P. "Exploiting the 60 GHz band for local wireless multimedia access: Prospects and future directions," *IEEE Communications Magazine*, No. 1, 140-147, Jan. 2002.
3. Anang, K. A., P. B. Rapajic, L. Bello, and R. Wu, "Sensitivity of cellular wireless network performance to system & propagation parameters at carrier frequencies greater than 2 GHz," *Progress In Electromagnetics Research B*, Vol. 40, 31-54, 2012.
4. Rappaport, B. T. S., J. N. Murdock, and F. Gutierrez, "State of the art in 60-GHz integrated circuits and systems for wireless communications," *Proceedings of the IEEE*, Vol. 99, No. 8, 1390-1436, 2011.
5. Cohn, S. B. and N. P. Weinhouse, "An automatic microwave phase measurement system," *Microwave Journal*, Vol. 7, No. 2, 49-56, 1964.
6. Engen, G. F. and C. A. Hoer, "Application of an arbitrary 6-port junction to power-measurement problems," *IEEE Transactions on Instrumentation and Measurement*, 470-474, 1972.
7. Engen, G. F., "An improved circuit for implementing the six-port technique of microwave measurements," *IEEE Transactions on Microwave Theory and Techniques*, Vol. 25, No. 12, 1080-1083, 1977.
8. Hoer, C. A., "The six-port coupler: A new approach to measuring voltage, current, power, impedance, and phase," *IEEE Transactions on Instrumentation and Measurement*, Vol. 21, No. 4, 466-470, 1972.
9. Engen, G. F., "The six-port reflectometer an alternative network analyzer," *IEEE Transactions on Microwave Theory Techniques*, Vol. 25, 1075-1077, 1977.
10. Li, J., K. Wu and R. G. Bosisio, "A Collision avoidance radar using six-port phase/frequency discriminator (SPFD)," *Proceedings of IEEE Microwave Theory and Techniques Symposium*, 1553-1556, 1994.
11. Li, J., R. G. Bosisio, and K. Wu, "Computer and measurement simulation of a new digital receiver operating directly at millimeter-wave frequencies," *IEEE Transactions on Microwave Theory and Techniques*, Vol. 43, No. 12, 2766-2772, Dec. 1995.

12. Li, J., R. G. Bosisio, and K. Wu, "Dual-ton calibration of six-port junction and its application to the six-port direct digital millimetric receiver," *IEEE Transactions on Microwave Theory and Techniques*, Vol. 44, No. 1, 93–99, 1996.
13. Tatu, S. O., E. Moldovan, K. Wu, and R. G. Bosisio, "A new direct millimeter-wave six-port receiver," *IEEE Transactions on Microwave Theory and Techniques*, Vol. 49, No. 12, 2517–2522, Dec. 2001.
14. Tatu, S. O., E. Moldovan, G. Brehm, K. Wu, and R. G. Bosisio, "ka band direct digital receiver," *IEEE Transactions on Microwave Theory and Techniques*, Vol. 50, No. 11, 2436–2442, Nov. 2002.
15. De la Morena-Álvarez-Palencia, C., M. Burgos-Garcia, and J. Gismero-Menoyo, "Four-octave six-port receiver and its calibration for broadband communications and software defined radios," *Progress In Electromagnetics Research*, Vol. 116, 1–21, 2011.
16. De la Morena-Álvarez-Palencia, C. and M. Burgos-Garcia, "Experimental performance comparison of six-port and conventional zero-IF/low-IF receivers for software defined radio," *Progress In Electromagnetics Research B*, Vol. 42, 311–333, 2012.
17. Tatu, S. O., E. Moldovan, K. Wu, R. G. Bosisio, and T. Denidni, "Ka-band analog front-end for software defined direct conversion receiver," *IEEE Transactions on Microwave Theory and Techniques*, Vol. 53, No. 9, 2768–2776, Sept. 2005.
18. Sarrazin, T., H. Vettikalladi, O. Lafond, M. Himdi, and N. Rolland, "Low cost 60 GHz new thin Pyralux membrane antennas fed by substrate integrated waveguide," *Progress In Electromagnetics Research B*, Vol. 42, 207–224, 2012.
19. Huang, T. Y. and T. J. Yen, "A high-ratio bandwidth square-wave-like bandpass filter by two-handed metamaterials and its application in 60 GHz wireless communication," *Progress In Electromagnetics Research Letters*, Vol. 21, 19–29, 2011.
20. Hannachi, C., D. Hammou, T. Djerafi, Z. Ouairi, and S. O. Tatu, "Complete characterization of novel MHMICs for V-band communication systems," *Journal of Electrical and Computer Engineering*, 1–8, Nov. 2013.
21. Hammou, D., E. Moldovan, K. Wu, and S. O. Tatu, "60 GHz MHMIC six-port model analysis," *Microwave and Optical Technology Letters*, Vol. 52, No. 9, Sept. 2010.
22. Williams, D. F., J. M. Belquin, G. Dambrine, and R. Fenton, "On-wafer measurement at millimeter wave frequencies," *IEEE MTT-S International Microwave Symposium Digest*, Vol. 3, 1683–1686, San Francisco, CA, Jun. 17–21, 1996.
23. Marks, R. B., "A multilayer method of network analyzer calibration," *IEEE Transactions on Microwave Theory and Techniques*, Vol. 39, 1205–1215, 1991.
24. Antsos, D., R. Crist, and L. Sukanto, "A novel Wilkinson power divider with predictable performance at K and Ka-band," *IEEE MTT-S International Microwave Symposium Digest*, 907–910, Jun. 1994.
25. Peters, F. D. L., D. Hammou, S. O. Tatu, and T. A. Denidni, "Modified millimeter-wave Wilkinson power divider for antenna feeding network," *Progress In Electromagnetics Research Letters*, Vol. 17, 11–18, 2010.
26. Hammou, D., E. Moldovan, and S. O. Tatu, "Novel ring millimeter wave power divider/combiner," *IEEE Canadian Conference on Electrical and Computer Engineering (CCECE 2011), Conference Proceedings*, 280–283, Niagara Falls, Ontario, May 8–11, 2011.
27. Hammou, D., T. Djerafi, M. Nedil, and S. O. Tatu, "Considerations for on-Wafer millimeter wave measurements on thin ceramic substrate," *IEEE Transactions on Instrumentation and Measurement*, Vol. 65, No. 2, 441–447, Nov. 2015.
28. Xu, Y. and R. G. Bosisio, "Wideband planar Goubau line (PGL) couplers and six-port circuits compatible with short range (60 GHz) radio," *IET Microwaves, Antennas & Propagation*, Vol. 7, No. 12, 985–990, 2013.
29. Talebzadeh, A. and A. Abdipour, "Miniaturized six-port receiver for 60 GHz communication," *IEEE 2014 22nd Iranian Conference on Electrical Engineering (ICEE)*, 1406–1410, 2014.

30. Zhang, J. and V. Fusco, "SiGe V-band 6-port receiver," *IET Seminar Millimeter Wave Technologies for Gigabit per Second Wireless Communications*, 51–60, Belfast, Sept. 2012.
31. Boukari, B., E. Moldovan, S. Affes, K. Wu, R. G. Bosisio, and S. O. Tatu, "A heterodyne six-port FMCW radar sensor architecture based on beat signal phase slope techniques," *Progress In Electromagnetics Research*, Vol. 93, 307–322, 2009.
32. Tatu, S. O. and E. Moldovan, "V-band multiport heterodyne receiver for high-speed communication systems," *EURASIP Journal on Wireless Communications and Networking*, Vol. 2007, No. 1, 45–45, 2007.
33. Hammou, D., N. Khaddaj Mallat, E. Moldovan, S. Affes, K. Wu, and S. O. Tatu, "V-band six-port down-conversion techniques," *International Symposium on Signals, Systems, and Electronics (ISSSE)*, conference CD, IEEE catalog Number 07EX1869C, 379–382, Montreal, Canada, 2007.
34. Texas Instruments, Inc., "THS4304-SP wideband operational amplifier (Rev. A)," *Data Sheet*, Jul. 2004.
35. Pozar, D. M., *Microwave and RF Design of Wireless Systems*, John Wiley and Sons, New York, 2001.
36. McKinley, M. D., K. A. Remley, M. Myslinski, J. S. Kenney, D. Schreurs, and B. Nauwelaers, "EVM calculation for broadband modulate signals," *NIST PML*, Tech. Rep., Gaithersburg, MD, 2005.